

# Microscopic Simulation of the Cardiac Electrophysiology: A Study of the Influence of Different Gap Junctions Models

Pierre-Elliott Bécue<sup>1,2,3</sup>, Mark Potse<sup>1,2,3</sup>, Yves Coudière<sup>1,2,3</sup>

<sup>1</sup> INRIA Bordeaux Sud-Ouest, Talence, France

<sup>2</sup> Institut de Mathématiques de Bordeaux, Talence, France

<sup>3</sup> Institut de Rythmologie et Modélisation Cardiaque, Pessac, France

## Abstract

*It has been suggested in the literature that a disorganization of cardiac tissue at the cellular scale may affect the propagation of the action potential (AP) at the tissue scale, and may play a role in arrhythmia.*

*We developed a model of the myocardium at sub-cellular resolution in which the intracellular space, the cell membrane, and the extracellular space are discretized individually [1]. We present in this article an improvement of this model, including gap junction models at any interface between cells. We then test this approach on hand-crafted two-dimensional networks of a hundred of cells, and compare it with our previous model which was not including gap junctions modelling.*

## 1. Introduction

The standard bidomain or monodomain equations model a cardiac tissue at the macroscopic scale. They may be derived by homogenization of microscopic bidomain equations, which model the propagation of the cardiac action potential (AP) on a network of individual cells. For homogenization, the network is assumed to be periodic.

Yet, dysfunction or disorganization (non periodicity) of the tissue at the cellular level may affect the propagation of the AP at the tissue scale. For instance, zigzag propagation at a cellular level has been hypothesized to lead to arrhythmias [2]. These alterations cannot be represented by the homogenized bidomain or monodomain models.

To understand and tackle such questions, we planned to simulate the bidomain equations written at the cellular scale on a manually designed network of cells. The equations were first studied theoretically [3], we proved existence of a solution (see ref.[4]), then we ran simulations on small handcrafted networks of individual cells [1].

In this paper we present an improved version of the equation system presented in ref.[1], that features gap junctions modelling. We describe briefly its properties,

and then compare the results it gives to the ones we got with the previous model.

## 2. The bidomain model at the cell scale

We consider a set of cells indexed from 1 to  $N$ . Each cell is a connected medium  $\Omega_i$ . The extracellular medium is noted  $\Omega_0$  and assumed to be connected. Each cell  $\Omega_i$  may be glued to some others. In such a case, the border between them is named  $\Gamma_{ij}$  (which is the same as  $\Gamma_{ji}$ ) where  $j$  is the index of the other cell. The border between a cell and the extracellular medium is  $\Gamma_{0i}$ . See example figure 1.

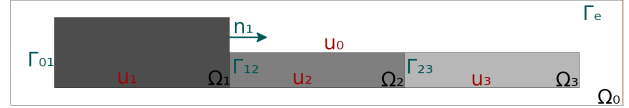


Figure 1. A 3-glued cells example describing the problem. The first cell is bigger because in our simulations, we want to be able to apply a stimulation on this cell without impacting the others.

For all time  $t > 0$ , the microscopic equations are  $-\nabla \cdot (\sigma_i \nabla u_i) = 0$  for all  $i \in \{0, \dots, N\}$ . The transmission conditions between two bordering media  $i$  and  $j$  is

$$-\sigma_i \nabla u_i \cdot n_i = \sigma_j \nabla u_j \cdot n_j = c_{ij} \partial_t v_{ij} + F_{ij}(v_{ij}, w_{ij}).$$

Last, there is a no-flux boundary condition  $\sigma_e \nabla u_e \cdot n_e = 0$  on the external boundary  $\Gamma_e$  of the system. Here,  $u_i$  denote potential fields in the cell  $i$  (or the extracellular medium 0).  $\sigma_i$  are scalar electrical conductivities for each medium. The trans-membrane voltage across  $\Gamma_{ij}$  is  $v_{ij} = u_i - u_j$ . Any border  $\Gamma_{ij}$  is modeled by a capacity  $c_{ij}$  in parallel with a ionic current  $F_{ij}$ . The vector  $w_{ij}$  defined on the interface gathers the additional state variables of such a ionic current model. Such model is either a classic ionic model when  $i$  or  $j$  is 0, or a gap junction model otherwise. We assume the initial data are given only for the trans-membrane voltages  $v_{ij}$ , as  $v_{ij}(0, x) = v_{ij}^0(x)$  for  $x \in \Gamma_{ij}$ .

There exists a well posed weak formulation of these equations, where  $u_i$  is searched in the space  $H^1(\Omega_i)$ , with an additional gauge condition for sake of uniqueness.

We approximate the solution with the P1-Lagrange finite element method, and use an Euler time-stepping method, implicit on the diffusion terms, and explicit on the ionic ones. Hence, for a sequence of times  $t^n = n\delta t$  ( $\delta t > 0$ ), we solve specific discrete equations on each  $u_i$  in the discrete P1 spaces, with the condition that the meshes of each domain (a cell, or the extracellular medium) coincides with the bordering other domains' ones.

For each time step, we have to solve a linear system of equations of the form  $AU^n = F^n$  where  $U^n = (U_0, \dots, U_N)^T$  is the vector of the degrees of freedom, and the right-hand side vector  $F^n = (F_0, \dots, F_N)^T$  involves the nonlinear functions  $F_{ij}$ .

### 3. Simulations and results

We intend to compare our results with the ones we got from our previous work in ref.[1]. Hence, we build two kind of problems. One type where the cells are connected by channels of intracellular material (see figure 2) (in a sense, there is only one long cell with local reductions that are channels), and one is with "glued" cells (see figure 3). The channels actually play a geometrical gap junction role, but this is far from realistic interpretations of gap junctions. In both figures, the "S" shape of the cell network is here for readability and also to respect the constraint that the extracellular medium has to be connected. On

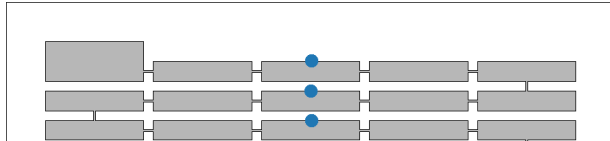


Figure 2. The top subset of a 100 cells network with channel junctions, before meshing. The blue dots are spots where we measure the potential variation across time. The whole network expands on 20 lines.

the glued case, each node on the membrane between two cells is assumed to be a gap junction. We will first test a linear gap junction model (Linear GJ), where the linear coefficient will be the conductance of the gap junctions (ie  $F_{ij}(v_{ij}, w_{ij}) = v_{ij}/R_{ij}$ ). Then, we will show results with a non-linear gap junction model extracted from experiments on mouse cells [5]. In the simulations, the intracellular conductivities are set to  $1.7\text{mS cm}^{-1}$  and the extracellular conductivity is set to  $3.0\text{mS cm}^{-1}$ . The membrane capacity is set to  $1\mu\text{F cm}^{-2}$ .

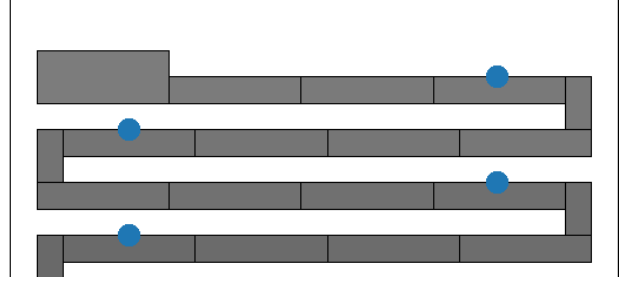


Figure 3. The top subset of a 99 glued cells network, before meshing. The blue dots are spots where we measure the potential variation on the membrane across time. The blackness of the cells is proportionate to their index (from 1 to 99). The whole network expands on 20 lines, the last lacking one cell compared to the others.

#### 3.1. Specificities of the linear system

The matrix of the linear system is symmetric, and is the addition of a stiffness matrix computed on all nodes, and two mass matrices, a first one extracted from the nodes on any border  $\Gamma_{ij}$ , and the other from coupling points between cells  $i$  and  $j$  who share a border. It is challenging to compute efficiently these matrices in our finite-element code, CEPS.

In addition, the initial problem is a pure Neumann equation (no-flux condition on the external boundary). Hence the linear system has a unique solution defined up to a constant. Here we compute the solution perpendicular to the kernel space of the matrix  $A$  (corresponding to a gauge condition) with a conjugate gradient iterative solver, as suggested in ref. [6].

#### 3.2. Computational solver and meshes

Our model was programmed in the software code CEPS developed at Inria. It relies on the PETSc library to solve the linear systems on parallel computers. In test cases below, the problems were designed via a Python script, and meshed using the Triangle meshing software. For our simulations, the channel-version of our meshes had 34k nodes, 67.6k triangles. The glued one had 32k nodes and 63.4k triangles.

#### 3.3. Comparison of the channel and the Linear GJ case

We chose a resistance value for the linear GJ case by iterative methods. Indeed, the bibliographic references always provide a resistance per area unit value. Here, in two-dimensions, we don't have any area value. Furthermore, we lack any intel on the gap junction density per unit of inter-cells membrane. We hence chose a value that was

giving reasonable action potential propagation velocities:  $0.015\text{k}\Omega$ . For each case, we run a simulation for 420ms, with a time step of 0.05ms, and an output each 0.1ms. In each case, we input a stimulation on each side of the left-upper cell, in order to depolarize it. This stimulation occurs at  $t = 20\text{ms}$ . For the Linear GJ case, the intensity of the stimulation is  $2.25 \times 10^{-5}\mu\text{A}$  for 0.15ms. For the channel case, the stimulation's intensity is  $2.70 \times 10^{-5}\mu\text{A}$ . This difference results from the fact that in the channel case, the diffusion implies the need for a bigger stimulation. We show in figures 4 5 the depolarization of the cells, measured on the blue dots shown in figures 2 and 3 respectively.

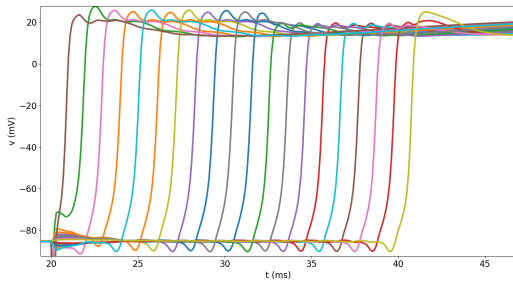


Figure 4. Potentials measured on the blue dots shown in figure 2 for the channel problem. The action potential takes 20ms to cross  $0.855\text{cm}$ , which gives a propagation speed of  $42.72\text{cm s}^{-1}$ , which is compatible with the expected AP velocity presented in the literature.

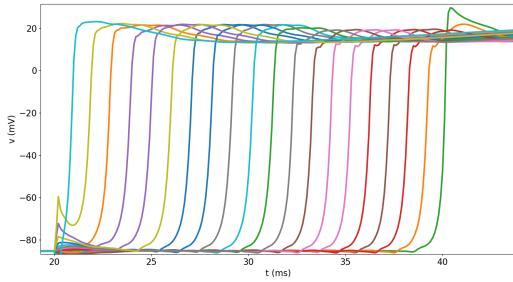


Figure 5. Potentials measured on the blue dots shown in figure 3 for the linear GJ problem. The action potential takes 19ms to cross  $0.817\text{cm}$ , which gives a propagation speed of  $43\text{cm s}^{-1}$ .

### 3.4. Linear GJ: influence of the resistance value on the AP velocity

In the following cases, we changed the value of the resistance for the gap junctions. We used six different resis-

tance values:  $R = 0.015\text{k}\Omega$ ,  $R = 0.03\text{k}\Omega$ ,  $R = 0.06\text{k}\Omega$ ,  $R = 0.075\text{k}\Omega$ ,  $R = 0.12\text{k}\Omega$ ,  $R = 0.15\text{k}\Omega$ . The outcome is that the higher the resistance, the lower the AP velocity. We show in figure 6 the velocity depending on the gap junctions resistance value.

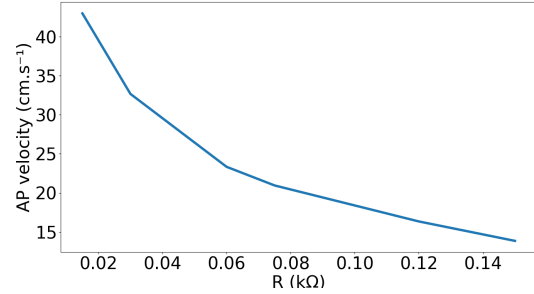


Figure 6. Presentation of the AP velocity depending on the resistance on the glued 99-cells problem with linear Gap Junctions. We see that the decrease of velocity is highly linked with the resistance of the Gap Junctions.

### 3.5. Linear GJ: influence of the GJ density on the AP velocity

Another question that arose during our studies is regarding whether a higher membrane-to-cross density on the path of the AP would significantly impact the AP velocity. To simulate such a behaviour, we designed a single-line network of a fixed length where the varying part was the length of a cell (and hence the number of cells, and hence the number of membranes to cross). We tested this problem with both the linear Gap Junction model and the non-linear one.

We chose to represent five cases: 10 cells of  $100\mu\text{m}$  length, 20 cells of  $50\mu\text{m}$  length, 50 cells of  $20\mu\text{m}$  length, 5 cells of  $200\mu\text{m}$  length and 2 cells of  $500\mu\text{m}$  length. On figure 7, we present the AP velocity depending on the typical cell's length. From this figure, we infer that the AP

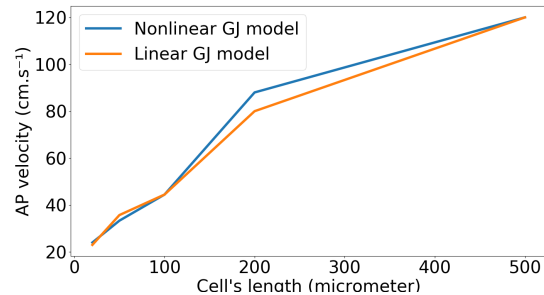


Figure 7. AP velocity depending on cell's length, and hence on the gap junction density.

velocity is impacted by the amount of Gap Junction the AP has to cross per unit of length. This tend to confirm the impact of the Gap Junctions on the propagation at the microscopic scale. To extract a reliable velocity intel for cells with great length (200 $\mu\text{m}$  or above), further testing with longer network should be done.

### 3.6. Example of non-linear GJ model

We implemented a non-linear GJ model from the results of ref.[5], that got derived from experimentations on rat heart cells. With the same parameters as the Linear GJ simulation, but replacing the linear GJ model by the previously mentioned model, we run a simulation. Figure 8 shows the potentials measured for this case. This result is not distin-

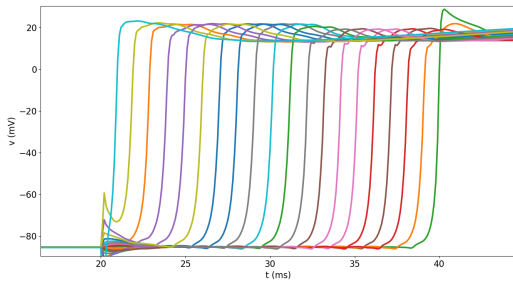


Figure 8. Potentials measured on the blue dots shown in figure 3 for the nonlinear GJ problem. The action potential takes 19ms to cross 0.817cm, which gives a propagation speed of 43cm s<sup>-1</sup>.

guishable from the linear problem with  $R = 0.015\text{k}\Omega$ .

### 3.7. Linear GJ: example with too high resistance on the membrane between two cells

We implemented a case where the resistance between two cells (the 38<sup>th</sup> and the 39<sup>th</sup>) is set to 1.5k $\Omega$ . Figure 9 shows the potentials measured on the blue dots in figure 3

## 4. Conclusion

From these different results we were able to show an impact of the gap junction modelling on the action potential velocity. The influence of the different models is to be explored further, with varying parameters, and methods, to confirm the above results. In particular, comparing simulation results with the experimental output from ref.[5] could provide a decent way to evaluate to what extend our model is realistic.

Yet, these results tend to answer positively to the questions regarding the influence of gap junctions modelling to

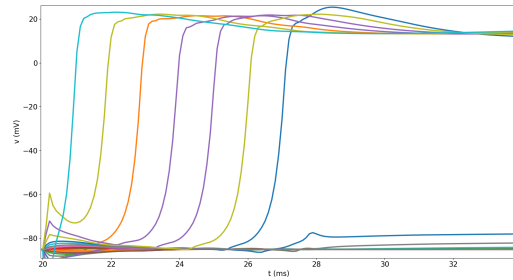


Figure 9. Potentials measured on the blue dots shown in figure 3 when  $R = 1.5\text{k}\Omega$  between the 38<sup>th</sup> and the 39<sup>th</sup> cells. We can see that the 39<sup>th</sup> cell failed to depolarize and came back to its resting potential.

get accurate intel regarding the electrical activities of the heart tissues when specific alterations occur. As homogenized model don't allow such studies, our model seems to provide a reasonable place to start.

## References

- [1] Bécue PE, Coudière Y, Potse M. A Three-Dimensional Computational Model of Action Potential Propagation Through a Network of Individual Cells. In Computing in Cardiology Conference (CinC). 2017; 1081–1084.
- [2] de Bakker JM, van Capelle FJ, Janse MJ, Tasseron S, Vermeulen JT, de Jonge N, Lahpor JR. Slow Conduction in the Infarcted Human Heart. 'Zigzag' Course of Activation. Circulation 1993;88(3):915–926. ISSN 0009-7322.
- [3] Colli-Franzone P, Savaré G. Degenerate Evolution Systems Modeling the Cardiac Electric Field at Micro- and Macroscopic Level. Basel: Birkhäuser Basel. ISBN 978-3-0348-8221-7, 2002; 49–78.
- [4] Bécue PE, Caro F, Potse M, Coudière Y. Theoretical and Numerical Study of Cardiac Electrophysiology Problems at the Microscopic Scale. SIAM Conference on the Life Sciences (LS16), July 2016. URL <https://hal.inria.fr/hal-01405837>. Poster.
- [5] Davidović A, Coudière Y, Desplantez T, Poinard C. Microscopic Modelling of the Non-Linear Gap Junction Channels. In 2015 Computing in Cardiology Conference (CinC). Nice, France, September 2015; URL <https://hal.inria.fr/hal-01418702>.
- [6] Bochev P, Lehoucq RB. On the Finite Element Solution of the Pure Neumann Problem. SIAM Review 2005;47(1):50–66.

Address for correspondence:

Pierre-Elliott Bécue  
Maison de la Simulation USR 3441, Bâtiment 565 - Digiteo,  
CEA Saclay, 91191 Gif-sur-Yvette cedex, France  
[pierre-elliott.becue@inria.fr](mailto:pierre-elliott.becue@inria.fr)